







## Virtual Reality Solutions for Enhanced Fault Diagnosis of Rolling Bearings in Passenger Cableways with an Improved Deep Learning Approach

Jun Zhang<sup>1\*</sup>, Hao Yu<sup>2</sup>, Xianxuan Zhang<sup>3</sup> and Juan Li<sup>4</sup>

<sup>1,2,3,4</sup>Qinghai Power Transmission and Transformation Engineering Co., Ltd.,  
Xining, Qinghai, 810001, China,  
[zhangjun123@mail.sdufe.edu.cn](mailto:zhangjun123@mail.sdufe.edu.cn), [13195796812@qq.com](mailto:13195796812@qq.com),  
[z\\_xuangq@163.com](mailto:z_xuangq@163.com), [lijuan66web@163.com](mailto:lijuan66web@163.com)

Corresponding author: Jun Zhang, [zhangjun123@mail.sdufe.edu.cn](mailto:zhangjun123@mail.sdufe.edu.cn)

**Abstract.** With the diversification, complexity, and intelligence of electromechanical equipment, the diagnosis and early warning of equipment failures have received widespread attention. Rolling bearings are important stress-bearing components of passenger ropeways, and their operating status will affect the overall smooth operation of the ropeway equipment. In the application of deep learning to fault diagnosis, two types of problems may arise: insufficient model training due to a shortage of fault samples imbalanced data, insufficient model generalization and reduced diagnostic accuracy due to differences in operating conditions and signal acquisition locations. To address these issues, a new fault diagnosis framework for rolling bearings based on deep convolutional generative adversarial networks (DCGAN) is proposed. The DCGAN architectures combined with a convolutional long-short-term memory network are used to ensure the extraction of time information of each time series data and related information between variables. In the proposed DCGAN, the input data distribution is learned, and the input signal is reconstructed using a generator subnetwork. The reconstructed signal is then dimensionally reduced using an encoder subnetwork, and the authenticity of both the input and output signals is determined using a discriminator subnetwork. Through the adversarial learning mechanism, the feature extraction of fault signals is completed, the generator is trained to learn the distribution characteristics of the original fault samples, and supplementary fault data samples are generated to establish a more accurate rolling bearing fault diagnosis model. The experimental results show that the proposed method can complete the fault diagnosis with high accuracy in the case of insufficient labeled data, which is helpful in improving the safety of the operation and maintenance of the cableway equipment.

**Keywords:** Passenger Ropeway; Rolling Bearing; Deep Learning; GAN; LSTM; Virtual Reality Solutions.

**DOI:** <https://doi.org/10.14733/cadaps.2024.S17.203-216>

## 1 INTRODUCTION

Passenger ropeway is one of the eight major types of special equipment, and it is a mechanical transportation facility that uses overhead ropes to support and pull passenger cars to transport passengers [1]. The advantages of the cableway include the fact that it can directly cross mountains and ground obstacles and has strong adaptability; the cableway has a short distance and can save travel time; its compact structure and small construction amount can reduce the damage to the natural landscape; its energy consumption is low (generally Powered by electricity) and non-polluting; its investment is relatively low compared to other forms of transportation, and the cost recovery time is shorter [3]. According to statistics, in 2019, China had 1,089 passenger ropeways, and the number of equipment was increasing year by year. However, some passenger cableways in China have been built and put into use for more than 10 years. The inspection and maintenance of passenger ropeways are basically based on traditional manual methods such as daily inspections, monthly inspections, annual inspections, and inspections of key components. Maintenance and repairs are still mainly based on regular maintenance and fault repairs. Manual regular repairs not only consume a lot of manpower, but also cause a waste of maintenance resources, and fault repairs have a certain lag. Often, faulty parts can only be repaired/replaced after equipment failures or accidents, bringing security risks to equipment operation [15].

Failure of rolling bearings will cause accidents and casualties [11]. However, due to its difficulty in disassembly, there is no mature and effective detection method at present, which brings huge safety hazards to the operation of the ropeway. In the past, the manual detection of cableway bearings was only to judge whether the bearings were faulty by observing whether there were abnormal noises and changes in temperature measurement values during operation. There is no standard that puts forward specific requirements for its non-destructive testing scheme, and there are huge potential safety hazards [5].

Since rolling bearings are subjected to loads for a long time during operation, they become one of the most vulnerable parts in machinery [6]. According to statistics, 30% of the failures of rotating machinery are caused by bearings. And in rolling bearing faults, 90% come from the inner races and outer races, and 10% come from rolling bodies and cages. Therefore, vibration and acoustic emission analysis are the most commonly used detection methods in research on fault detection of rolling bearings worldwide [22]. The traditional rolling bearing fault diagnosis method mainly includes two steps. First, the sensors are used to collect the bearing vibration signals, and then a series of signal processing-based techniques are used to extract fault features for fault diagnosis [2]. However, this type of analysis method has high requirements for signal processing algorithms and professional knowledge. At the same time, different fault severity or complex on-site working conditions will lead to the low signal-to-noise ratio of the collected vibration signals, making it difficult to achieve high-precision fault diagnosis. Under actual working conditions, the vibration signals of bearing faults are relatively weak and are easily covered by strong interference signals. Specifically, Virtual Reality (VR) solutions, coupled with an advanced deep learning approach, represent a transformative paradigm in the field of fault diagnosis. This convergence not only addresses the complexities associated with maintenance challenges but also elevates the standards of efficiency and precision in identifying issues within rolling bearings.

The application of machine learning algorithms in bearing fault diagnosis mainly consists of three parts: fault feature extraction, feature selection, and fault classification [17]. The feature extraction of bearing faults is mainly to extract the fault features in the vibration signals for

subsequent analysis. At present, the commonly used methods for preprocessing the vibration signals of bearing faults include envelope analysis, spectral kurtosis, wavelet transform, EMD, VMD, etc [10]. After selecting the features extracted by the above techniques, they are used as the training samples of the classification algorithm for classification. Such methods mainly focus on how to extract effective fault features as training samples for classification algorithms to improve the reliability and accuracy of bearing fault diagnosis. Wang et al. [19] proposed a fault feature extraction method based on wavelet packet decomposition (WPD) and local mean decomposition (LMD) permutation entropy and used the extracted feature vector as a training sample for support vector machine (SVM) for training classification. Qing et al. [21] used EMD to process vibration signals and extract features for low-speed rolling bearing faults and used the extracted fault features as the input of the PSO-LSSVM model for classification and diagnosis. On the basis of EMD and abstract energy operator, Li et al. [12] proposed a method based on phase difference correction to improve the identification accuracy of faulty bearing frequencies. In order to solve the problems of information loss or excessive decomposition of vibration signals, Li et al. [14] used the VMD algorithm to extract weakly coincident features, and the similarity of envelopes is utilized to reconstruct the signals, effectively solving the problems of noise interference and over-decomposition

With the continuous development and improvement of Deep Learning (DL) algorithms, they have gradually replaced machine learning algorithms and have been widely used in various fields. The DL algorithm mainly maps the extracted data features to a new feature space by building a deep network and continuously iterating between network layers. Through the continuous mapping of feature information, the features are continuously abstracted between layers, and the automatic extraction of bearing fault features is realized through the nonlinear activation function set in each layer of the network, getting rid of the dependence on manual intervention and expert experience [7]. Hasan et al. [8] preprocessed the collected fault signals based on the discrete orthogonal Stockwell transform, and used them as the input of the Convolutional Neural Network (CNN) for training and classification; Xie et al. [20] used discrete wavelet transform to extract features of the collected bearing vibration signals and then trained the CNN network. However, the above methods still use manual feature extraction for the input of CNN, which fails to fully realize the powerful self-learning ability of CNN network, which limits the improvement of fault diagnosis accuracy. Moreover, the vibration signal of the bearing collected by the sensor is a one-dimensional time series signal, and the data points at adjacent moments are highly correlated. If it is converted into a two-dimensional form and used as the input of the CNN network for training, it will easily destroy the correlation between the original data, resulting in loss of some fault information. In addition, the above methods require a large amount of labeled data in model training, and it is difficult to obtain labeled operating data under actual working conditions.

In order to solve the problem of sparse labeling data for rolling bearings, Li et al. [13] proposed an improved Generative Adversarial Network (GAN) model, and cross-domain fault diagnosis is accomplished by generating artificial samples under fault conditions. Gao et al. [4] proposed a method based on the Wasserstein GAN (WGAN) with gradient penalty for insufficient sample data, and redesigned the loss function of WGAN. Shao et al. [18] utilized a 1D CNN to construct an auxiliary classifier GAN for data augmentation, where the additional label information is beneficial to generate corresponding failure samples.

The above GAN-based data generation methods can still reconstruct and restore data in the case of high dimensionality and a large proportion of information loss. However, due to the limitation of the loss function, GAN will experience gradient disappearance and dispersion during the training process. Although the improved WGAN method can solve the gradient disappearance problem to a certain extent, it will lead to a decrease in training efficiency.

For this reason, this paper proposes a fault diagnosis method for rolling bearings of passenger ropeway based on improved Deep Convolutional GAN (DCGAN) and Convolutional LSTM (Conv-LSTM). The main contributions of the proposed method include: 1) The improved DCGAN is used in the field of fault diagnosis of cableway bearings, and combined with the Conv-LSTM network to achieve accurate extraction of time information and spatial information of fault features, which significantly enhance the model's ability to distinguish faulty signals from normal signals. 2) In model training, through the mechanism of adversarial learning, the feature information of the fault signals is extracted and the distribution of fault data is approximated, and the generator is used to obtain artificial fault data samples to solve the problem of unbalanced training samples.

The remainder of this paper is organized as follows. Section I gives an introduction to the working principle of classic GAN for anomaly detection. Section II explains the proposed non-destructive fault diagnosis method for rolling bearings of passenger ropeway based on improved DCGAN and Conv-LSTM. Section II gives the experimental results and analysis. Finally, Section IV summarizes the full text and proposes future research directions.

## 2 RESEARCH BACKGROUND

### 2.1 GAN Model

GAN models are structurally inspired by game theory. Strictly speaking, a GAN framework consists of at least two parts, one is the generator  $G$ , and the other is the discriminator  $D$ . Its basic structure is shown in Figure 1.

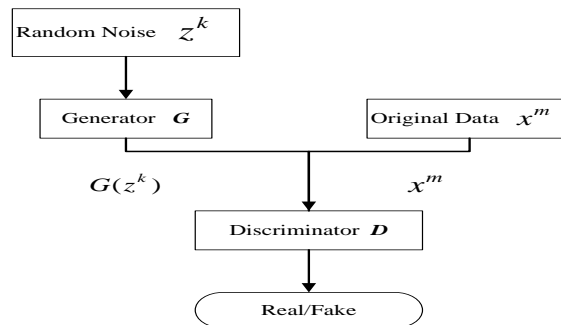


**Figure 1:** Anomaly detection principle of GAN.

Generator  $G$  and discriminator  $D$  are generally formalized by neural network structures. The generator  $G$  captures the underlying distribution of real data samples and generates new artificial data samples. During training, real data samples and generated data samples are randomly sent to the discriminator  $D$ . The discriminator  $D$  is a binary classifier, which aims to identify real samples to the greatest extent and pick out generated artificial samples. The goal of the generator is exactly the opposite of that of the discriminator. It needs to reduce the probability of the generated samples being recognized by the discriminator as much as possible, thus forming an adversarial training mechanism. In this way,  $G$  and  $D$  form a minimum-maximum game, and the loss function of GAN can be described as [9]:

$$\min_G \max_D \left\{ f(D, G) = E_{x \sim P_{\text{dat}}(x)} [\ln D(x)] + E_{z \sim P_z(z)} [\ln (1 - D(G(x)))] \right\} \quad (1)$$

where  $x$  denotes real data;  $z$  is a random vector or random noise;  $P_{data}$  is the real data sample distribution;  $G(z)$  is the sample data generated by the generator  $G$  that follows the real data distribution  $P_{data}$  as much as possible, that is, fake sample data. The two sides optimize themselves during the iterative adversarial training process and jointly improve performance until a balance is reached. When the discriminator  $D$  cannot correctly identify the source of the data (that is, it cannot distinguish between real and fake samples), then it is concluded that the generator  $G$  has learned the sample distribution of real data.

## 2.2 Conv-LSTM

LSTM can transfer past information to current data and mine the relationship between adjacent sequence data. Therefore, LSTM can be used to extract relevant information between sequential data. The traditional LSTM network is fully connected layer by layer, but the convolution operation can obtain more structural information. In order to learn spatial information and local structural information, Yuan et al. [23] proposed to use a network that combines convolution operations and LSTM, called ConvLSTM. ConvLSTM is constructed by adding an LSTM-based convolution operation, which is a convolutional connection between layers. The structure of ConvLSTM is the same as that of classic LSTM, and the convolution operation of each gate in the LSTM unit replaces the fully connected operation with a convolution operation. The structure information of adjacent inputs is fed back to the current data through convolution operation. Moreover, the features extracted by convolution are transmitted to the next layer to obtain more information. Figure 2 shows the structure diagram of ConvLSTM.

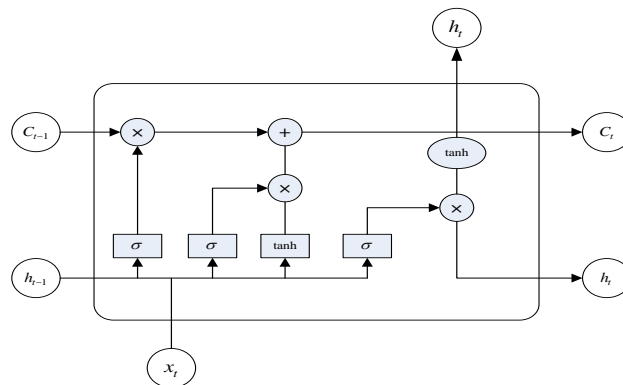


**Figure 2:** Internal structure of Conv LSTM.

ConvLSTM can capture spatial features and transfer them to adjacent inputs by following the update equation, and utilizes three gating layers to control memory access. The internal structure is calculated as follows:

$$i_t = \sigma(W_{xi} * x_t + W_{hi} * H_{t-1} + W_{ci} * C_{t-1} + b_i) \quad (2)$$

$$f_t = \sigma(W_{xf} * x_t + W_{hf} * H_{t-1} + W_{cf} * C_{t-1} + b_f) \quad (3)$$

$$C_t = f_t \circ C_{t-1} + i_t \circ \tanh(W_{xc} * x_t + W_{hc} * H_{t-1} + b_c) \quad (4)$$

$$o_t = \sigma(W_{xo} * x_t + W_{ho} * H_{t-1} + W_{co} * C_t + b_o) \quad (5)$$

$$H_t = o_t \circ \tanh(C_t) \quad (6)$$

Where  $\circ$  denotes Hadamard operation;  $*$  denotes convolution operation;  $\sigma$  is the activation function;  $x_t$  is the input tensor;  $H_t$  is the hidden state tensor;  $C_t$  is the memory unit tensor;  $W_x$  and  $W_h$  correspond to 2D convolution kernels for input and hidden states, respectively;  $b_i$ ,  $b_f$ ,  $b_c$ , and  $b_o$  are bias terms.

### 3 ANOMALY DETECTION SCHEME OF ROLLING BEARING OF PASSENGER CABLEWAY BASED ON IMPROVED DEEP LEARNING MODEL

#### 3.1 Anomaly Detection Model Combining ConLSTM and GAN

The model proposed in this paper is composed of 4 parts, namely the discriminator  $D$ , the first encoder  $Enc1$ , the second encoder  $Enc2$  and the decoder  $Dec$ . Figure 3 shows the structure of the proposed model.

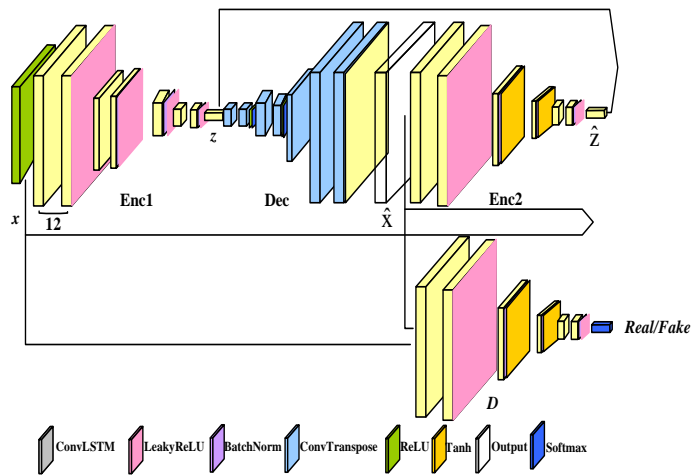


**Figure 3:** Structure of the proposed model.

In Figure 3, the first sub-network is an autoencoder network consisting of encoder 1 (Enc1) and decoder (Dec) as the generator  $G$  of the model. The generator learns the input data distribution and reconstructs the input signal by using encoder and decoder networks, respectively. The sub-network works as follows: the generator  $G$  first reads the input signal  $x$ , and forwards it to its encoding network Enc1. By using a ConvLSTM layer followed by Batch Norm and LeakyReLU activation functions in turn, Enc1 performs dimensionality reduction on  $x$  by compressing  $x$  to a vector  $z$ .  $z$  is also known as the bottleneck feature of the generator  $G$  and is assumed to be the best representation containing the smallest dimensionality of  $x$ . The decoder part of the generator network Dec adopts the generator architecture of DCGAN, using convolution transposition layer, ReLU activation function, Batch Norm normalization and tanh layer at the end. This technique amplifies the vector  $z$  to reconstruct the input signal  $x$  as  $\hat{x}$ . Thus,  $x$  is fed to the first encoder to get  $z = Enc1(x)$ , and then  $z$  is passed to the decoder network to get  $\hat{x} = Dec(z)$ .

The second subnetwork is the Encoder 2 (Enc2), which is used to compress the signal  $\hat{x}$  reconstructed by the generator  $G$ . It has the same structural details as Enc1. Enc2 performs

dimensionality reduction on  $\hat{x}$  to find the corresponding feature  $\hat{z} = \text{Enc2}(\hat{x})$ . For consistent comparisons, the vector  $\hat{z}$  has the same dimension as  $z$ . The latent vector is minimized by bottleneck features, and learned how to use the minimum distance to achieve feature representation.

The third sub-network is the discriminator  $D$ , which aims to classify the input  $x$  and the output  $\hat{x}$  as true or false, respectively. In GAN, the discriminator plays a very important role. Based on the continuous adversarial training of the discriminator network and the generator network, the generator network can finally reach the Nash equilibrium and obtain the best parameters to simulate the original distribution of the data. If the discriminator is not strong enough or the structure is unstable, it may lead to the failure of the entire GAN network. This subnetwork is the standard discriminator network introduced in DCGAN [16].

The specific structure of Encoder 1 uses a 3-layer Conv-LSTM model to extract the temporal and spatial features of samples. Encoder 1 reads the input  $x$  through a sub-network including Conv-LSTM layer, Batch Norm layer and LeakyReLU activation function, and outputs the latent feature  $z$  (bottleneck feature).  $z$  is used as the unique representation of the input  $x$ . Symmetrically to Encoder 1, the decoder network upsamples the latent feature  $z$  until it is of the same dimension as the input signal and reconstructs the output, denoted as  $\hat{x}$ . Encoder 2 and discriminator adopt the same structure as Encoder 1, but their respective parameters are learned independently during training. The Encoder 1 and decoder form a generalized generator, which together with the discriminator form a GAN.

### 3.2 Fault Diagnosis Process

In order to monitor and diagnose the health status of cableway rolling bearings while distinguishing the authenticity of the samples, the discriminator not only recognizes the state patterns of the samples, but also outputs the true/false labels of the samples. The generator generates corresponding new data samples  $X_{\text{fake}} = \{x_{\text{fake}}^k\}_{k=1}^K$  based on the input sample labels, and inputs it together with the original samples as a training set to the discriminator, and then the discriminator outputs the true/false labels of the samples associated with the corresponding fault type labels.

Let the category label error and the true/false label error be the loss functions, and iteratively train the generator and the discriminator alternately. The process is as follows:

When using the generator to generate new samples, Gaussian noise is randomly sampled to obtain random vectors  $\{z^k\}_{k=1}^K$ , which are fed into the generator and mapped to  $h_z^k$  (hidden layer vectors), and then new samples  $\{x_{\text{fake}}^k\}_{k=1}^K$  are generated with corresponding category labels. The calculations are as follows:

$$h_z^k = f_{\theta_z}(W_z z^k + b_z) \quad (7)$$

$$x_{\text{fake}}^k = f_{\theta'_z}(W'_z h_z^k + b'_z) \quad (8)$$

Where  $\theta_z$  represents the input layer to the hidden layer of the neural network,  $\theta_z = \{W_z, b_z\}$ ;  $\theta'_z$  is the parameter set from the hidden layer to the output layer of the neural network,  $\theta'_z = \{W'_z, b'_z\}$ ;  $W_z$  and  $W'_z$  are weight matrices.

During discriminator training, it is assumed that new samples  $\{\mathbf{x}_{fake}^k\}_{k=1}^K = 0$  are generated, corresponding to the real category labels  $y_{fise}^k$ , and the original samples are  $\{\mathbf{x}^m\}_{m=1}^M = 1$ , corresponding to the real category labels  $y_m$ .  $y_{fate}^k$  and  $y_m$  are input to the discriminator for authenticity discrimination, and the corresponding fake/real labels  $\mathbf{d}_{real}^m$ ,  $\mathbf{d}_{fake}^k$ , along with the associated category labels  $c_{real}^m$  and  $c_{fake}^k$  are output. The discriminator network is trained by minimizing the error of the true and false labels and the error of the category labels. The loss functions are calculated as follows:

$$L_c = -\frac{1}{M} \sum_{m=1}^M [y^m \ln c_{real}^m + (1 - y^m) \ln (1 - c_{real}^m)] - \frac{1}{K} \sum_{k=1}^K [y_{fake}^k \ln c_{fake}^k + (1 - y_{fake}^k) \ln (1 - c_{fake}^k)] \quad (9)$$

$$L_d = -\frac{1}{M} \sum_{m=1}^M \ln \mathbf{d}_{real}^m - \frac{1}{K} \sum_{k=1}^K \ln (1 - \mathbf{d}_{fake}^k) \quad (10)$$

$$L_D = \underset{\Theta}{\operatorname{argmin}} (L_c + L_d) \quad (11)$$

where  $L_D$  is the loss function of the discriminator in DCGAN;  $\Theta$  denotes the parameter set;  $L_d$  is cross-entropy loss error of the true/false labels;  $L_c$  is the cross-entropy loss error of the category labels.

### 3.3 Sample Generation and Fault Diagnosis Algorithm

The original fault samples are used to train DCGAN, and the feature information in the fault signal is extracted through the mechanism of adversarial learning, and the distribution of the fault data is approximated. The final generator is considered to have learned the distribution of the original fault samples. In this way, theoretically speaking, the generator can be used to obtain new fault data samples to supplement the original fault data samples and solve the problem of sample imbalance. The algorithm implementation process is shown in Figure 4.

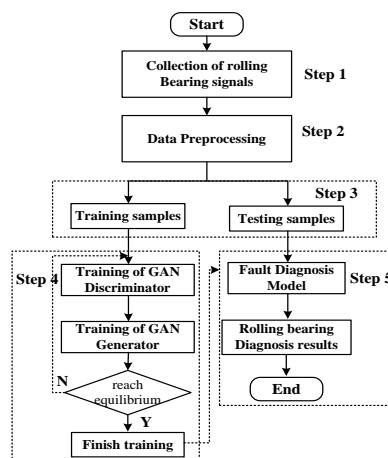


Figure 4: Fault diagnosis process of the proposed method.

## 4 EXPERIMENTS AND ANALYSIS

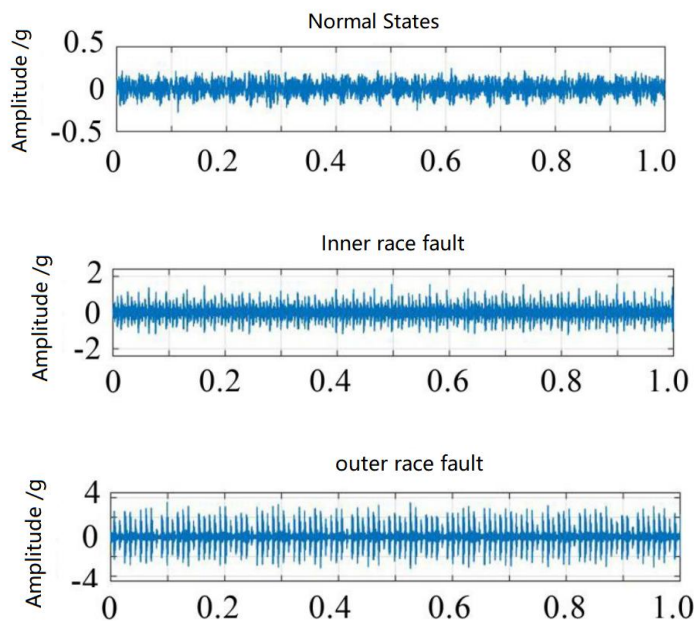


#### 4.1 Dataset Description

In order to verify the effectiveness of the proposed fault diagnosis method for passenger cableway rolling bearings based on the improved deep learning model, the bearing dataset from the Case Western Reserve University (CWRU) of the United States is used as the experiment dataset, and the effectiveness of the proposed fault diagnosis method is verified. Four types of bearings with inner race fault, outer race fault, rolling body fault and normal state are selected as the experimental objects. The signal was collected under four different operating speed conditions (1 797 r/min, 1 772 r/min, 1 750 r/min and 1 730 r/min, respectively), and the sampling frequency was 12 kHz. Table 1 gives the dataset details, and Figure 5 shows the time-domain schematic diagram of different fault signals. It can be seen from Figure 5 that although the vibration signals of different types of faults have their own characteristics, it is difficult to observe the fault features hidden in the vibration signals. The ratio of labeled data to unlabeled data samples contained in the experimental data set is 1:6.5, that is, the amount of unlabeled data in the experimental data far exceeds that of labeled data, and the amount of labeled data is less than that used in general machine learning. Therefore, the dataset can fully verify the data labeling ability and fault classification ability of the proposed method.

<i>Bearing States</i>	<i>Normal States/ Sample number</i>	<i>Inner race fault/ sample number</i>	<i>Outer race fault/ sample number</i>	<i>Rolling body fault/ sample number</i>
	- / 4571	0.41 mm / 865	0.35 mm / 866	0.41 mm / 866
<i>Pitting diameter</i>	0.18 mm / 1085	0.54 mm / 864	0.54 mm / 865	0.55 mm / 865
<i>/mm</i>	-	0.66 mm / 865	0.16mm / 866	-
	-	0.17 mm / 865	-	-

**Table 1:** Statistics of the experiment dataset.



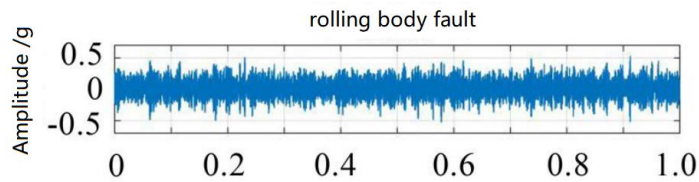


Figure 5: Time domain diagram of normal signals and fault signals.

## 4.2 Configuration of the Deep Learning Model

Simulation experiments are performed in a Python environment to evaluate the fault detection and classification performance of the proposed method. The hardware platform is Intel i5-7500 3.5 GHz CPU, 8 GB RAM, NVIDIA GeForce GTX 960 GPU. The experiment is implemented on TensorFlow2.2, optimized by Adam optimizer, the initial learning rate is  $2e-3$ , momentum  $\beta_1=0.5$ ,  $\beta_2=0.999$ . The hidden layer of Conv-LSTM is set to  $h = 250$ , and the number of training rounds is set to 2000 according to experience. When the performance of the model begins to decline, the parameters of the network are saved, because this performance decline is a sign of overfitting.

## 4.3 Evaluation Metrics

To evaluate the fault diagnosis performance of the proposed method, accuracy (Acc), precision (Pre), recall (Rec) and F1 (F1) scores are used as performance metrics, which are calculated as:

$$Acc = \frac{TP}{N} \quad (12)$$

$$Pre = \frac{TP}{TP+FP} \quad (13)$$

$$Rec = \frac{TP}{TP+FN} \quad (14)$$

$$F_1 = 2 \times \frac{Pre \times Rec}{Pre + Rec} \quad (15)$$

where  $N$  is the actual number of samples in the category,  $TP$  is the number of samples that actually belong to category  $c$  and are correctly classified into category  $c$ ,  $FP$  indicates the number of samples that actually do not belong to category  $c$  but are incorrectly classified into category  $c$ ,  $FN$  is the number of samples that actually belong to category  $c$  but are misclassified into other categories. The F1 score is the harmonic mean of recall and precision, and the closer the value is to 1, the better the performance.

## 4.4 Ablation Study

The proposed method incorporates the Conv-LSTM model into the classic DCGAN network to better capture and distinguish fault signal features. ConvLSTM is used to enhance the ability to capture temporal and spatial features, and follow the update equation to transfer them to adjacent inputs, thereby improving the overall sensitivity of the model to fault signals. Table 2 shows the average of the comparison results of the proposed method and the traditional DCGAN on the test data set for 5 experiments. It can be found that the proposed method achieves a better fault detection performance, and the average accuracy of the proposed method in 5 experiments is 96.17%, which is significantly higher than the average accuracy of 87.13% with traditional DCGAN. From

the experimental results, it can be seen that the proposed improved deep learning model and training optimization method have higher diagnostic efficiency in fault diagnosis.

<i>Models</i>	<i>Acc</i>	<i>Pre</i>	<i>Rec</i>	<i>F1</i>
<i>Classic DCGAN</i>	<i>75.13</i>	<i>76.77</i>	<i>80.15</i>	<i>78.42</i>
<i>Proposed Method</i>	<i>96.17</i>	<i>96.12</i>	<i>98.32</i>	<i>97.21</i>

**Table 2:** Ablation analysis results (/%).

#### 4.5 Comparison Results

Table 3 shows the comparison results of the proposed method and the methods proposed in [12], [18] and [19] in terms of accuracy and F1 score on the experimental dataset. The data used in the proposed method and the comparison method are all original time-domain signals. In order to avoid the influence of chance, each method uses the same parameters to conduct 5 experiments and take the mean value. Among them, PSO-LSSVM [12] is a machine learning method based on manual features, and its fault classification performance cannot meet the requirements of safe operation of the cableway. In comparison with other deep learning methods, the proposed method achieves the highest accuracy and F1 score, because the proposed method uses the LSTM network to extract the context information of the long-term span of the data, and on this basis, it can also extract the spatial information with the DCGAN network, that is, the information between each attribute dimension. Therefore, the proposed model has an accuracy of 96.12% for fault classification, and an F1 score of 97.21%, which is the best among all methods for anomaly detection. It is proved that the proposed method has higher diagnostic accuracy and better stability when dealing with a large amount of unlabeled data.

	<i>Pre (/%)</i>				<i>F1 score (/%)</i>			
	<i>[12]</i>	<i>[18]</i>	<i>[19]</i>	<i>Proposed method</i>	<i>[12]</i>	<i>[18]</i>	<i>[19]</i>	<i>Proposed method</i>
<i>Inner race fault</i>	<i>55.35</i>	<i>85.77</i>	<i>87.19</i>	<i>97.65</i>	<i>50.27</i>	<i>82.55</i>	<i>87.10</i>	<i>98.02</i>
<i>Outer race fault</i>	<i>55.21</i>	<i>83.91</i>	<i>86.77</i>	<i>96.99</i>	<i>53.46</i>	<i>81.43</i>	<i>86.60</i>	<i>97.68</i>
<i>Rolling body fault</i>	<i>49.79</i>	<i>77.34</i>	<i>86.29</i>	<i>93.78</i>	<i>44.38</i>	<i>80.97</i>	<i>85.89</i>	<i>95.93</i>
<i>Average</i>	<i>53.45</i>	<i>82.34</i>	<i>86.75</i>	<i>96.12</i>	<i>49.37</i>	<i>81.65</i>	<i>86.43</i>	<i>97.21</i>

**Table 3:** Comparison results of fault classification.

Figure 6 shows the accuracy results of the proposed method, classic CGAN, and other advanced methods in five repeated experiments. It can be seen from the figure that the proposed method achieves the highest accuracy in all five experiments, and has better stability than other algorithms.

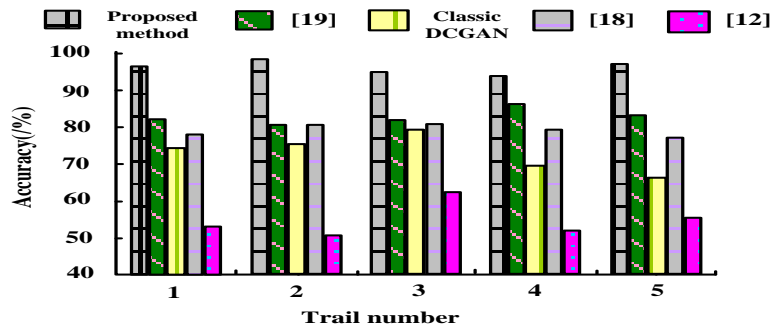


Figure 6: Accuracy results in five experiments.

## 5 CONCLUSION

Fault diagnosis of rolling bearings is a research hotspot in the field of mechanical fault diagnosis. In order to solve the problems of difficult access to labeled data samples, unstable models during training, and difficulty in setting parameters in traditional intelligent diagnosis methods, the improved DCGAN is used in the field of fault diagnosis in this paper. Firstly, an improved DCGAN anomaly detection model is proposed. Aiming at the problem of fault diagnosis under the condition of unbalanced sample data, a diagnosis model is established. Secondly, the experimental platform is used to simulate and collect rolling bearing data in various state modes, and the signal processing and fault diagnosis experiment analysis is carried out. Finally, the results obtained by the proposed method and other advanced deep learning methods are compared and summarized, and the results verify the effectiveness of the proposed method in extracting fault features and the intelligence of efficient fault identification. The comparison of experimental results shows that compared with other advanced methods, the proposed method has higher accuracy and good stability, and can complete the fault data labeling task while classifying with high precision, which has certain engineering application prospects. In the follow-up work, we will further think about how to improve the design network structure, so as to further improve the precision and recall rate of the model. In addition, we will also try to use advanced visualization technology to more intuitively display the fault diagnosis results of the deep learning-based model.

Jun Zhang, <https://orcid.org/0009-0004-2693-8539>

Hao Yu, <https://orcid.org/0009-0000-8452-6920>

Xianxuan Zhang, <https://orcid.org/0009-0007-7446-4763>

Juan Li, <https://orcid.org/0009-0008-4351-8412>

## REFERENCES

- [1] Camargo, Pérez, J.; Carrillo, M. H.; Montoya-Torres, J. R.: Multi-Criteria Approaches for Urban Passenger Transport Systems: A literature Review, *Annals of Operations Research*, 226, 2015,69-87. <https://doi.org/10.1007/s10479-014-1681-8>

- [2] Cerrada, M.; Sánchez, R. V.; Li, C.: et al. A Review on Data-Driven Fault Severity Assessment in Rolling Bearings, *Mechanical Systems and Signal Processing*, 99, 2018,169-196. <https://doi.org/10.1016/j.ymssp.2017.06.012>
- [3] Ferrarese, M.; Loner, E.; Pulina, M.: Demand, Business Profitability and Competitiveness in the Cableway System: A multidimensional framework, *Research in Transportation Economics*, 2021, 2021, 90, 101041. <https://doi.org/10.1016/j.retrec.2021.101041>
- [4] Gao, X.; Deng, F.; Yue X.: Data Augmentation in Fault Diagnosis Based on the Wasserstein Generative Adversarial Network with Gradient Penalty, *Neurocomputing*, 396, 2020, 487-494. <https://doi.org/10.1016/j.neucom.2018.10.109>
- [5] Gawroński, W. P.: Design of the Aerial Cableway Supporting Structure Located in the Terrain of the TatryZachodnie in InstytutInżynieriiBudowlanej, 2019.
- [6] Guo, R.; Wang, Y.; Zhang, H.: et al. Remaining Useful Life Prediction for Rolling Bearings Using EMD-RISI-LSTM, *IEEE Transactions on Instrumentation and Measurement*, 70, 2021, 1-12. <https://doi.org/10.1109/TIM.2021.3051717>
- [7] Hakim, M.; Omran, A. A. B.; Ahmed, A. N.: et al. A Systematic Review of Rolling Bearing Fault Diagnoses Based on Deep Learning and Transfer Learning: Taxonomy, overview, application, Open Challenges, Weaknesses and Recommendations, *Ain Shams Engineering Journal*, 2022, 101945. <https://doi.org/10.1016/j.asej.2022.101945>
- [8] Hasan, M. J.; Kim, J. M.: Bearing Fault Diagnosis Under Variable Rotational Speeds Using Stockwell Transform-Based Vibration Imaging and Transfer Learning, *Applied Sciences*, 8(12), 2018, 2357. <https://doi.org/10.3390/app8122357>
- [9] Jiang, W.; Hong, Y.; Zhou, B.: et al. A GAN-Based Anomaly Detection Approach for Imbalanced Industrial Time Series *IEEE Access*, 7, 2019, 143608-143619. <https://doi.org/10.1109/ACCESS.2019.2944689>
- [10] Kirankumar, M. V.; Loksha, M.; Kumar, S.: et al. Review on Condition Monitoring of Bearings Using vibration Analysis Techniques in IOP Conference Series: Materials Science and Engineering, IOP Publishing, 376 (1), 2018, 012110. <https://doi.org/10.1088/1757-899X/376/1/012110>
- [11] Knawa-Hawryszków, M.: Determining Initial Tension of Carrying Cable in Nonlinear Analysis of Bi-Cable Ropeway–Case Study, *Engineering Structures*, 2021, (244), 2021, 112769. <https://doi.org/10.1016/j.engstruct.2021.112769>
- [12] Li, X.; Xie, Z.; Luo, J.: Application of the Phase Difference Correct Method in Rolling Bearing Fault Diagnosis, *Journal of Algorithms & Computational Technology*, 11, (4), 2017, 378-387. <https://doi.org/10.1177/1748301817725313>
- [13] Li, X.; Zhang, W.; Ding, Q.: Cross-Domain Fault Diagnosis of Rolling Element Bearings Using Deep Generative Neural Networks, *IEEE Transactions on Industrial Electronics*, 66, (7), 2022, pp. 5525-5534. <https://doi.org/10.1109/TIE.2018.2868023>
- [14] Li, Z.; Chen, J.; Zi, Y.: et al. Independence-Oriented VMD to Identify Fault Feature for Wheel Set Bearing Fault Diagnosis of High-Speed Locomotive, *Mechanical Systems and Signal Processing*, 85, 2017, 512-529. <https://doi.org/10.1016/j.ymssp.2016.08.042>
- [15] Martinod, R. M.; Bistorin, O.; Castañeda, L. F.: et al. Maintenance Policy Optimisation for Multi-Component Systems Considering Degradation of Components and Imperfect Maintenance Actions, *Computers & Industrial Engineering*,124, 2018,100-112. <https://doi.org/10.1016/j.cie.2018.07.019>
- [16] Salimans, T.; Goodfellow, I.; Zaremba, W.: et al. Improved Techniques for Training Gans, *Advances in neural information processing systems*, 2016, (29), 2016.
- [17] Schwendemann, S.; Amjad, Z.; Sikora, A.: A Survey of Machine-Learning Techniques for Condition Monitoring and Predictive Maintenance of Bearings in Grinding Machines, *Computers in Industry*, 2021, (125) 2021, 103380. <https://doi.org/10.1016/j.compind.2020.103380>

- [18] Shao, S.; Wang, P.; Yan, R.: Generative Adversarial Networks for Data Augmentation in Machine Fault Diagnosis, *Computers in Industry*, 106, 2019, 85-93. <https://doi.org/10.1016/j.compind.2019.01.001>
- [19] WANG, M.; MIAO, B.; YUAN, C.: Adaptive Bearing Fault Diagnosis based on Wavelet Packet Decomposition and LMD Permutation Entropy, *International Journal*, 2016, (4), 2016.
- [20] Xie, Y.; Zhang, T.: Feature Extraction Based on DWT and CNN for Rotating Machinery Fault Diagnosis in 2017 29th Chinese Control And Decision Conference, *IEEE*, 2017, 3861-3866. <https://doi.org/10.1109/CCDC.2017.7979176>
- [21] Xiong, Q.; Xu, Y.; Peng, Y.: et al. Low-Speed Rolling Bearing Fault Diagnosis Based on EMD Denoising and Parameter Estimate with Alpha Stable Distribution, *Journal of Mechanical Science and Technology*, 4, 2017,1587-1601. <https://doi.org/10.1007/s12206-017-0306-y>
- [22] Xu, Y.; Zhen, D.; Gu, J. X.: et al. Autocorrelated Envelopes for Early Fault Detection of Rolling Bearings, *Mechanical Systems and Signal Processing*, 2021, (146), 2021, 106990. <https://doi.org/10.1016/j.ymssp.2020.106990>
- [23] Yuan, Z.; Zhou, X.; Yang, T.: Hetero-convlstm: A Deep Learning Approach to Traffic Accident Prediction on Heterogeneous Spatio-Temporal Data in *Proceedings of the 24th ACM SIGKDD International Conference on Knowledge Discovery & Data Mining*, *IEEE Press*, 2018, 984-992. <https://doi.org/10.1145/3219819.3219922>